Research Square

Preprints are preliminary reports that have not undergone peer review.
They should not be considered conclusive, used to inform clinical practice,
or referenced by the media as validated information.

Unveiling microbial complexity within Astragalus propinquus and Glycyrrhiza uralensis roots

Zerrin KOZMA KIM

kozmazerrin@snu.ac.kr

Seoul National University https://orcid.org/0000-0001-9694-955X

Young Sang Park

Seoul National University

Tae-Jin Yang

Seoul National University

Hyun Kim

Seoul National University https://orcid.org/0000-0002-7322-713X

Yong-Hwan Lee

Seoul National University https://orcid.org/0000-0003-2462-1250

Research Article

Keywords: Endophytic fungi, Endophytic bacteria, Astragalus propinquus, Root microbiome, Glycyrrhiza uralensis

Posted Date: January 17th, 2025

DOI: https://doi.org/10.21203/rs.3.rs-5675838/v1

License: This work is licensed under a Creative Commons Attribution 4.0 International License.
Read Full License

Version of Record: A version of this preprint was published at Annals of Microbiology on May 17th, 2025. See the published version at https://doi.org/10.1186/s13213-025-01802-0.

Abstract

Background

Astragalus propinquus (*AP*) and *Glycyrrhiza uralensis* (*GU*), members of the Fabaceae family, are widely used for their therapeutic properties. However, the endophytic microbial communities in their roots remain largely unknown. Herein, we compared the structure and properties of root-associated bacterial and fungal communities of *AP* and *GU*, specifically excluding the microbial communities thriving in the rhizosphere, using both culture-dependent and -independent methods.

Results

A metabarcoding-based approach revealed a higher abundance of *Proteobacteria* in the root microbiome of *GU* than in that of *AP*. Fungal communities showed similar distinctions, with *AP* and *GU* predominantly harboring *Ascomycota* and *Basidiomycota*, respectively. The bacterial community in *AP* exhibited significantly higher diversity than in *GU* and included unique taxa, e.g., *Steroidobacterales* and *Micromonosporales*. However, the bacterial community in *GU* was relatively less diverse and dominated by *Xanthomonadales*. Differential abundance analysis revealed that the plant species significantly impacted 301 bacterial and 228 fungal amplicon sequence variants (ASVs) in *AP* and *GU*. Among these, B5_f_*Comamonadaceae* was markedly more enriched in *AP* than in *GU*. A random forest model analyzing bacterial ASVs with significant differences in abundance indicated that most bacterial ASVs were enriched in *AP*. A pan-microbial community of 1,243 ASVs was identified, including 96 co-detected ASVs between *AP* and *GU*, with 3 core ASVs (B2_f_*Pseudomonas*, B5_*Comamonadaceae*, and B70_*Cutibacterium*). The fungal community comprised 435 ASVs, with 98 shared ASVs and 8 core ASVs (F5_*Paraphoma*, F6_f_*Lysurus*, F22_*Alternaria*, F30_*Phaeosphaeria*, F53_*Cladosporium*, F36_*Moesziomyces*, F55_f_*Neocucurbitaria*, and F56_*Malassezia*). Hub nodes were identified to elucidate the roles of microorganisms within microbial networks. In *AP*, B152_o_*Burkholderiales*, F14_*Exophiala*, and F33_*Fusarium* were the key hub nodes, whereas, in *GU*, B36_*Paenibacillus* was the central hub node. The comparative analyses of *in vitro* culture data and molecular sequencing results showed overlapping patterns, with *Pseudomonas* dominant in *AP* and *Bacillus* in *GU*.

Conclusions

These findings highlight distinct microbial communities between *AP* and *GU*, with each species exhibiting unique bacterial and fungal orders and differences in microbial network complexity and diversity. These differences suggest the potential functional contributions, e.g., nutrient cycling and secondary metabolite production, of root-associated microbial communities, likely impacting the therapeutic properties of these plants.

Introduction

In nature, microbes and plants interact and evolve together (Lebeis, 2014; Müller et al., 2016). A growing number of studies have proven that microbes form symbiotic relationships with their hosts and that these intimate connections have developed and adapted to enable these tight interactions (Hassani et al., 2018; Uroz et al., 2019). Moreover, plants need microbiota for their growth and development (Chaparro et al., 2014; Chaparro et al., 2012; del Carmen Orozco-Mosqueda et al., 2018), stress resistance (Bakker & Mercado-Blanco, 2012; Marasco et al., 2012), and sustained economic growth (Kudjordjie et al., 2019; Turner et al., 2013).

Endophytes are a unique class of plant microbiota (Hassani et al., 2018; Uroz et al., 2019) that inhabit and colonize internal plant niches. There is evidence that plant endophytes can boost therapeutic chemical production, support plant development, and protect host plants against pathogen invasion (Deng & Cao, 2017; Oono et al., 2015). Plant microbiome have been linked to the buildup of plant secondary metabolites (Li, Yang, et al., 2021; Zhang et al., 2020). These interactions highlight the critical role of microbiomes in shaping the phytochemical properties of plants. The functional variances revealed in rhizospheric microbiomes and endophytes demonstrate their potential resemblance to the therapeutic properties of conventional herbal remedies (Huang et al., 2018). The similarities between bioactive compounds derived from herbal remedies and the functional traits of rhizospheric microbiomes have sparked interest in elucidating the interactions between different therapeutic plant species and their microbiomes. Elucidating the composition and functional roles of endophytic bacteria and fungi within root niches is crucial for exploring their biotechnological applications, particularly in the context of the synthesis of secondary metabolites, which are considered a source of potential natural medicines and are crucial to the pharmacologic value of medicinal plants (Masand et al., 2015). Endophytic microbes, including fungi and bacteria, are known to contribute to the synthesis of pharmacologically relevant secondary metabolites in medicinal plants. Prior studies have provided the evidence of the involvement of these endophytes in partial and complete metabolic pathways, contributing to the synthesis of plant metabolites (Brader et al., 2014; Ludwig-Müller, 2015). For instance, *Paraphoma* species, commonly found in root tissues, are associated with the production of terpenoids, compounds with known anti-inflammatory properties. Similarly, in the plants of *Swietenia mahagoni* (*L.*) *Jacq*, *Cladosporium* species have been reported to synthesize phenolic compounds, which exhibit antioxidant activity (Chandra et al., 2024). Moreover, huperzine, known for its potential therapeutic effects in Alzheimer's disease and other memory disorders, is produced by the endophytic fungus *Shiraia* sp. Slf14, isolated from *Huperzia serrata* (Zhu et al., 2010). Moreover, complex interactions within the plant-associated microbiomes contribute to various plant traits, whereas individual microbial species play distinct roles in secondary metabolite production. These relationships highlight the multifaceted nature of plant–microbe interactions (Trivedi et al., 2020).

Medicinal plants are widely recognized for their therapeutic bioactive compounds, which have been extensively studied for their health benefits. The accumulating evidence of the critical role of plant microbiomes in enhancing these therapeutic effects has made it essential to not only study these medicinal plants but also their interactions with their microbiomes. *Astragalus propinquus* [*AP*, syn. *Astragalus membranaceus* (Fisch.) Bunge] and *Glycyrrhiza uralensis* (*GU*) represent a rich source of

therapeutic compounds (Asl & Hosseinzadeh, 2008; Xu et al., 2006) and, both species are renowned for their medicinal properties (Chung et al., 2001; Liu & Lv, 2020; Stickel & Schuppan, 2007; Sun et al., 2012). The microbiome of *AP*, for instance, has been shown to harbor a diverse array of bacteria and fungi that contribute to the production of crucial secondary metabolites, such as polysaccharides and saponins (Sun et al., 2017). Similarly, the microbiome of *GU* has been reported to enhance the bioavailability and potency of the flavonoid and phenolic compounds produced in this species (Ji et al., 2016). Despite their common family lineage, these plants exhibit distinct phytochemical profiles believed to be partially impacted by their unique microbial communities (Bratkov et al., 2016; Liu et al., 2023). Both plants occupy a significant position in traditional Korean medicine and remain the subjects of considerable interest in modern pharmacological research. Currently, there is relatively less knowledge regarding microbial communities in the roots of *AP* and *GU* that have a potential to impact the phytochemical properties of medicinal plants.

In this study, we aimed to conduct an in-depth examination of the diversity and composition of microbial communities in the roots of *AP* and *GU* plants. Specifically, beyond elucidating the complex nature of microbiomes, the aim is to determine the differences between the structure and associations of their bacterial and fungal communities using culture-independent and -dependent methods. The taxonomic composition of microbial communities in the roots of *AP* and *GU* may provide crucial insights into the biosynthesis of plant secondary metabolites, such as glycyrrhizin in *GU* and astragalosides in *AP*.

Materials and Methods

Experimental design and sample preparation

The fresh whole roots of *AP* and *GU* plants were collected from the Care Farm in Iksan, South Korea (36°00'12.7"N 127°03'51.8"E), in March 2022, when *AP* and *GU* were in the vegetative growth stage. We acquired each of the two species of medicinal plants from a single site that most optimally represents the species to reduce the impact of environmental variations and highlight the role of genetic factors. The plants of *AP* and *GU* were morphologically identified by Prof. Tae-Jin Yang and Young Sang Park of the Department of Agriculture, Forestry and Bioresources, Seoul National University (Seoul, Korea). Three individual plant roots (at least 30 cm long) collected from each plant were kept in sterile plastic bags, placed into an ice box, and then transported to the laboratory within 24 h. All samples were stored at 4°C until DNA extraction. Root samples were washed under running tap water to remove bulk soil and then surface-sterilized sequentially for 1 min, 3 min, and 30 s with 75% ethanol, 5% NaOCl, and 75% ethanol, respectively. Approximately 1 cm long root segments were excised from the samples for subsequent analyses. The root segments were then transferred to lysing matrix S tubes included in the SPINeasy DNA Kit for Soil (MP Biomedicals, USA). Each tube contained three root segments to ensure sufficient DNA amount to be used for further analyses. To consider the variability in root microbiomes within each individual, eight analytic replicates (randomly selected two or three replicates for each individual) were prepared. All treated root samples were kept in 1X phosphate-buffered saline (PBS), pH 7.4, to avoid DNA denaturation.

DNA extraction and molecular analyses

The prepared samples were ground using a homogenizer (FastPrep-24™ 5G; MP Biomedicals, USA). DNA was extracted following the manufacturer's instructions. All DNA samples were quality-checked and measured using a NanoDrop spectrophotometer (Thermo Fisher Scientific, USA). The extracted DNA was subjected to polymerase chain reaction (PCR) utilizing the primer set 799F–1193R for the V5–V7 region of the bacterial 16S ribosomal RNA (rRNA) gene (Bulgarelli et al., 2012), and the ITS1 regions of the fungal rRNA genes were amplified by ITS1-F/R and ITS2-F/R PCR primers (Op De Beeck et al., 2014). The reaction mix consisted of 12.5 μL of 0.5 μM 2× Platinum SuperFi II Green PCR Master Mix (Thermo Fisher Scientific, USA), 1 μL each of 0.5 μM forward and reverse primers, and 0.8 μM of diluted DNA template. PCR was performed using the following program for 16S rRNA: initial denaturation at 98°C for 30 s, followed by 32 cycles of denaturation at 98°C for 10 s, primer annealing at 55°C for 10 s, and extension at 72°C for 40 s, final extension at 72°C for 5 min, and holding at 12°C. For the PCR amplification of fungal ITS regions, the same procedure was followed. The MEGAquick-spin Plus DNA Purification Kit (iNtRON Biotechnology, Korea) was used to pool and purify amplicon replicates obtained from the same DNA sample. The sequencing was performed at Seoul National University's National Instrumentation Center for Environmental Management.

Sequence processing and statistical analyses

QIIME2 (v.2020.2) was used to process the sequencing reads (Bolyen et al., 2019). After demultiplexing, the sequences were combined and quality-filtered in the QIIME2 pipeline using the DADA2 plugin (Callahan et al., 2016). Amplicon sequence variants (ASVs) were then allocated to the processed reads. Non-chimeric ASV taxonomic classifications were assigned using the Nave Bayes technique, which is implemented in the q2-feature-classifier program (Bokulich et al., 2018). The taxonomies for the V5–V7 region of the 16S rRNA gene were based on the SILVA database (v.138) (Quast et al., 2012). The taxonomic designations for the ITS regions were performed using the UNITE database (UNITE_ver8_dynamic of May 2021) (Nilsson et al., 2019). Bacterial sequences with lengths ranging from 278 to 400 bp and fungal sequences ranging from 100 to 400 bp were included. The R package phyloseq was used to clean the ASV profiles (McMurdie & Holmes, 2013). These filtering techniques reduced the overall ASV count in bacteria to 1,339 and in fungi to 435. The ASVs designated as "kingdom Fungi" but unable to be recognized at the phylum level were subjected to a BLASTn search. The ensuing BLAST results were examined for plant sequences and those discovered were eliminated. In addition, chloroplasts and mitochondria were removed from the bacterial ASV profile. For all statistical analyses performed in R version 4.2.2 (R Core Team, 2013), the statistical significance threshold was set at $p = 0.05$. The cumNorm function in the R package metagenomeSeq (v. 3.8) was used to log-transform the ASV database and normalize it using cumulative-sum scaling (Paulson et al., 2013). The Chao1, Observed operational taxonomic unit (OTU), Shannon, Inverse Simpson, and Simpson indices were calculated using the alpha diversity function in the R package vegan (v2.5-3) (Oksanen, 2014). In addition, all Wilcoxon rank-sum tests were performed using the R software. The Bray–Curtis dissimilarity

matrix was computed to generate primary coordinate analyses with and without restrictions. Constrained principal coordinate analyses (PCoAs) were performed using the phyloseq and vegan package functions. The adonis2 function from the vegan package (v2.5-3) (Oksanen, 2014) was used for the permutational multivariate analysis of variance (PERMANOVA). The permutest function of the vegan package was used to perform variance partitioning and significance analysis for experimental variables with 99,999 permutations. Using the FitZig function of the metagenomeSeq package, a zero-inflated Gaussian distribution mixture model was developed to examine the disparities in abundance between the bacterial and fungal ASVs. The makeContrasts and eBayes commands were developed using the R package limma (v.3.34.9) (Ritchie et al., 2015). The false discovery rate (FDR)-adjusted *p*-values were checked to establish the statistical significance of the differences in abundance, and those with values less than 0.01 were deemed significant. Volcano plots generated using ggplot2 were used to visualize the ASVs with various degrees of bacterial and fungal abundances. The parameters for the random classification model, which included the two species, i.e., *AP* and *GU*, were set based on the abundance of microbiota. The ROCR (v. 1.0.7) and randomForest packages (v. 4.6–14) were used for this task, and the final machine learning strategy utilizing the random forest (RF) model in R was used to investigate receiver operating characteristic curves (Liaw & Wiener, 2002). The average reduction in the Gini coefficient was used to evaluate the relevance of the ASVs in assessing how well the RF model predicted *AP* and *GU* and was performed using the significance function from the randomForest package. The top ASVs from the RF models of each kingdom were classified as *AP*_enriched and *GU*_enriched or non-differential ASVs based on the results of the differential abundance test. Taxa with a relative abundance greater than 0.5% were represented for taxonomic composition analysis using the R program ggplot2 (Wickham, 2009). The core ASVs for both medicinal plants were found. A prevalence criterion of 90 and 95% was specified for core bacterial and fungal ASVs, respectively.

Microbial network analyses

iNAP was mostly used in the selection process (Feng et al., 2022). The input data for the SparCC analysis was sourced from the combined bacterial and fungal ASV abundance tables (Friedman & Alm, 2012). The estimated correlations ($p = 0.05$, two-sided) only included correlations for which the absolute coefficient values were ≥ 0.3 (Kurtz et al., 2015). The ForceAtlas2 layout was utilized for visualization using Gephi (v0.9.2) (Bastian et al., 2009). Degree, betweenness, closeness, and eigenvector centralities were calculated using R and Gephi (v0.9.2) (Bastian et al., 2009). The top 1% of degree and closeness centralities in each network were chosen as the hub nodes.

Isolation of bacteria and fungi from root samples

Surface-sterilized root samples were homogenized using a FastPrep-24TM 5G homogenizer (MP Biomedicals, USA), and the resulting root slurries were serially diluted 10-fold. The root samples were taken from the pooled and sterilized segments, and for each plant species, three replicates of 1 g of root tissue were homogenized in sterile PBS. The subsamples (0.1 µL) of each dilution were plated in

triplicate onto ISP medium No. 5 (ISP5), ISP medium No. 2 (ISP2), starch agar, egg yolk agar (EYA), Luria–Bertani agar (LB), trypticase soy agar (TSA), and Reasoner's 2A agar (R2A) agar for bacterial cultivation and yeast peptone dextrose adenine (YPDA), MEDION potato dextrose agar (MPDA), potato dextrose agar (PDA), rose bengal agar (RBA), and Sabouraud dextrose agar (SDA) for fungal cultivation. In addition, each medium used for bacterial or fungal cultivation contained 0.1 g L^{-1} cycloheximide or chloramphenicol to inhibit fungal or bacterial growth, respectively. Plates were incubated in a growth incubator for 2–7 days at 25 and 28°C for bacterial and fungal cultivation, respectively, following which colonies were counted, and final counts were expressed as CFU g^{-1} root. Microbial DNA was extracted from selected individual colonies to ensure a diverse and representative dataset. For bacterial isolation, seven different culture media (ISP5, ISP2, STARCH, EYA, LB, TSA, and R2A) were used, whereas five media (YPDA, MPDA, PDA, RBA, and SDA) were employed for fungal isolation. Colonies were selected based on their morphological diversity, with priority given to those displaying distinct morphotypes on the respective media. Additionally, colonies exhibiting robust and consistent growth were chosen to maximize diversity within the dataset.

Identification of bacterial and fungal isolates

The bacterial and fungal DNA samples were extracted and purified using the PURE gDNA Extraction Kit (Infusion Tech, Korea). A PCR mix of total volume 20 µL containing 1 µL DNA, 1 µL of each primer, 10 µL of 2X TOP Simple DyeMIX Taq master mix, and 7 µL of ddH_2O was used for each PCR amplification. The PCR reactions were performed using the following protocol: initial denaturation at 95°C for 2 min, followed by 34 cycles of denaturation at 95°C for 30 s, primer annealing at 55°C for 60 s, and extension at 72°C for 100 s, final extension at 72°C for 5 min, and holding at 12°C. The amplified PCR products were verified with electrophoresis on a 1% agarose gel containing SafeView (Applied Biological Materials, Canada) to determine their sizes (~500 bp) and approximate concentrations and purified using a MEGAquick-spin plus fragment DNA purification kit (iNtRON Biotechnology, Korea). The bacterial amplified PCR products were sequenced using the sequencing primers 515R (TTACCGCGGCTGCTGGCA), 926F (AAA CTCAAAGGAATTGACGG) (Lane, 1991), and 1055R (AGCTGACGACAGCCAT) (Lee et al., 1993) and assembled using the SeqMan Lasergene software version 7.1.0 (DNAStar, Madison, WI, USA). The similarity of the 16S rRNA gene sequence with those of known bacterial type strains was determined using the EzBioCloud server (Yoon et al., 2017). The pure cultures of the obtained microorganisms were established and stored at − 80°C for long-term storage as glycerol stocks. For the sequencing of fungal amplified PCR products, the ITS1 (TCCGTAGGTGAACCTGCGG) and ITS4 (TCCTCCGCTTATTGATATGC) primers were used (White, 1990). PCR was performed with initial denaturation at 95°C for 2 min, followed by 34 cycles of denaturation at 95°C for 30 s, primer annealing at 55°C for 30 s, and extension at 72°C for 90 s, final extension at 72°C for 5 min, and holding at 12°C. The process was the same for the PCR amplification of bacterial DNA.

Results

Microbial community composition and diversity varies in AP and GU

We examined the makeup of bacterial and fungal communities at the level of the same family but different genera, i.e., *AP* and *GU*, by comparing the relative and the estimated absolute abundances of dominant bacterial and fungal phyla associated with the root. The examination of taxonomic affiliations revealed variations in the dominance of orders across both medicinal plants (Supplementary file: Figures S1 and S2). Specifically, in the bacterial communities of *AP* and *GU*, *Proteobacteria* emerged as the predominant phylum, with the order *Pseudomonadales* (46%) in *AP* and the order *Xanthomonadales* (41.6%) in *GU* leading in average relative abundance. *Rhizobiales* ranked as the second most dominant bacterial community in both plant species, with the abundances of 15 and 36.3%, respectively. Notably, *AP* housed seven bacterial orders not found in *GU* (*Steroidobacterales*, *Cytophagales*, *Micromonosporales*, *Nevskiales*, *Streptosporangiales*, *Glycomycetales*, and *Acidimicrobiales* at 0.3, 0.2, 0.1, 0.1, 0.072, 0.066, and 0.062%, respectively), whereas *GU* exhibited two unique orders absent in *AP* (*Chlamydiales* and *Bacteroidales* at 0.22 and 0.01%, respectively) (Fig. 1a; Table S1). This compositional difference was also found in the fungal community, where Ascomycota (*Pleosporales*, 26.75%) predominated in *AP*, and Basidiomycota (*Phallales*, 52.1%) in *GU*. However, in both *AP* and *GU*, the order *Boletales* from the phylum *Basidiomycota* (32 and 68% in *AP* and *GU*, respectively) exhibited a significant presence, with 25 and 14.7% relative abundances, respectively (Fig. 1b). In *AP*, three distinct fungal orders were identified that were not present in *GU* (*Thelebolales*, *Sordariales*, and *Helotiales* at 0.6, 0.2, and 0.1%, respectively). In contrast, *GU* exhibited a unique fungal order (*Ustilaginales*, 0.7%) absent in *AP* (Fig. 1b; Table S1). *AP* and *GU* differed significantly in terms of their bacterial communities and dominant fungal communities. *AP* exhibited a diverse bacterial community and was mostly dominated by A*scomycota* in the fungal domain. In contrast, *GU* was characterized by the dominance of certain bacterial taxa, such as *Xanthomonadales*, and the dominance of *Basidiomycota* in the fungal kingdom.

The observed composition patterns further supported the differences in community diversity. The alpha diversity of root microbial communities was assessed using the Shannon, Observed OTU, Inverse Simpson, Chao1, and Simpson indices (Fig. 1c, d). For the bacterial community, *AP* showed significantly higher diversity than that in *GU* (Shannon, $P = 0.01$; Inverse Simpson, $P = 0.005$) (Fig. 1c). In addition, richness (Observed OTU, $P = 0.06$; Chao1, $P = 0.08$) and evenness (Simpson, $P = 0.06$) were higher in *AP* than in *GU*; however, the difference was not statistically significant. Regarding the fungal community, *GU* exhibited greater richness than that in *AP* (Observed OTU, $P = 0.008$; Chao1, $P = 0.007$) (Fig. 1d). However, there were no significant differences in the diversity and evenness indices (Shannon, $P = 0.4$; Inverse Simpson, $P = 0.8$; Simpson, $P = 0.4$). The combined results of PCoA and PERMANOVA showed that the bacterial and fungal communities were significantly different between the two plant species (bacteria: $R^2 = 0.25$, $P = 0.0001$; fungi: $R^2 = 0.22$, $P = 0.0001$) (Fig. 1e, f; Table S2). These results suggest that plant genetic or physiological factors may drive the differentiation of root endophytic bacterial and fungal communities between *AP* and *GU* under identical environmental conditions.

Differential distribution of root-associated microbiotas in AP and GU

As we found compositional differences among the medicinal plants of *AP* and *GU*, we aimed to seek distinct microbial taxa contributing to the observed composition patterns. The differential abundance analysis showed that, for *AP* and *GU*, 301 bacterial and 228 fungal ASVs, were significantly affected by the plant species (log_2 fold change > 2 or < − 2, FDR-adjusted $P < 0.01$). B5_f_*Comamonadaceae* was notably more abundant in *AP* than in *GU*, whereas B1862_f_*Sphingomonadaceae* exhibited a significantly higher abundance in *GU* that in *AP*. F1_*Fusarium*, a fungus, was relatively more enriched in *AP* than in *GU* (Fig. 2a, b; Table S3). As the differential abundance analysis could overrepresent the differences in abundance between the two plant species, we constructed two RF classification models for each domain to complement this limitation. These RF models were used to select the top 20 ASVs based on the similarity in their cross-validation error rates with those of the RF models (Table S4). Additionally, their importance in predicting the target variable was determined using the Gini uncertainty measure. In *AP* and *GU*, the top 20 bacterial ASVs (Fig. 2c) consisted of *Proteobacteria* (15 ASVs), and *Actinobacteria* (5 ASVs). Among the bacterial ASVs showing significant differences in abundance distribution, most bacterial ASVs were enriched in *AP*. Among the fungal ASVs showing significant differences in abundance distribution, most fungal ASVs were "*AP*-enriched," except for the six "GU-enriched" ASVs (Fig. 2d).

Core ASVs of the root microbiome of AP and GU

As *AP* and *GU* plants were grown under the same environmental conditions, we next aimed to examine the presence of common bacterial or fungal taxa which exist in both plant species. Therefore, we adopted the concept of core ASVs, which refer to species consistently found and plentiful in different samples or settings. To find the conserved fraction, we identified core ASVs with > 90% (bacteria)/95% (fungi) for *AP* and *GU* (Fig. 3). In the bacterial community, a pan-microbial community consisting of 1,243 ASVs were identified, including 96 co-detected ASVs between *AP* and *GU*, of which, only 3 ASVs were identified as core ASVs (B2_f_*Pseudomonas*, B5_*Comamonadaceae*, and B70_*Cutibacterium*) (Fig. 3a). Within the fungal community, the eight major fungal taxa, i.e., F5_*Paraphoma*, F6_f_*Lysurus*, F22_*Alternaria*, F30_*Phaeosphaeria*, F53_*Cladosporium*, F36_*Moesziomyces*, F55_f_*Neocucurbitaria*, and F56_*Malassezia*, were identified as the prevalent core ASVs (Fig. 3b). Although these bacterial and fungal taxa existed in both plant species, their abundance patterns differed across both species (Fig. 3). In particular, B2_f_*Pseudomonas*, B5_*Comamonadaceae*, F5_*Paraphoma*, and F6_f_*Lysurus* were relatively more abundantly distributed in *AP*. These results highlight that there may be common plant factors that help core ASVs colonize the root endosphere, and *AP* may provide relatively more appropriate niche environments to certain core taxa than offered by *GU*.

Network analysis of endophytic microbial communities in the root microbiomes of AP and GU

We constructed the microbial networks of both *AP* and *GU* to gain a comprehensive understanding of the complex and dynamic associations of root endophytic microbial communities. There were 80 bacterial and 42 fungal nodes and 565 connections (321 positive and 244 negative associations) for *AP*, whereas, for GU, there were 48 bacterial and 53 fungal nodes and 601 connections (374 positive and 227

negative associations) with a threshold set as the correlations of > 0.3 and < − 0.3 ($P < 0.05$) (Fig. 4a–d). In the *AP* network, fungi showed significantly higher connectivity than that exhibited by bacteria (degree, $P = 0.04$; closeness centrality, $P = 0.12$), whereas, in the *GU* network, bacteria exhibited higher connectivity than that exhibited by fungi (degree, $P = 0$; closeness centrality, $P = 0$) (Fig. 4b–e). To obtain a clear impression of the roles of microorganisms in these microbial networks, hub nodes were identified using degree and closeness centrality measures, and nodes falling within the top 1 percentile in these measurements were considered the hub nodes. In *AP*, B152_o_*Burkholderiales*, F14_*Exophiala*, and F33_*Fusarium* were identified as the hub nodes (Fig. 4c). In *GU*, B36_*Paenibacillus* was defined as the hub node (Fig. 4f). Moreover, the possibility of common associations between the networks of *AP* and *GU* reveals a significant overlap between these networks. The high correlation values of the common associations in the two networks indicate that the majority of these associations are statistically significant (pseudo-$P < 0.05$) (Table S5). The predominance of positively correlated associations suggests that biological similarities and functional connections between these networks are strong. These results support that networks of *AP* and *GU* are shaped under similar environmental or biological processes.

Comparison of ASVs and culture-dependent molecular identification methods

To confirm the significance of the key microorganisms associated with *AP* and *GU*, as identified based on culture-independent studies, we employed a culture-dependent approach to isolate root microorganisms. The isolates acquired from the cultures were subjected to BLAST analysis to determine if they matched the bacterial and fungal species known to be positively associated with *AP* and *GU*. The stringent selection criteria applied during isolation aimed to ensure the purity and distinctiveness of the colonies, focusing on their unique morphotypes and strong growth on the selective media. Notably, during storage at − 80°C, some bacterial and fungal strains may be well preserved, whereas others may be adversely affected by the storage conditions, potentially contributing to the reduced number of successful isolates. Therefore, we analyzed 55 morphologically distinct bacterial and 13 fungal isolates from *AP* and *GU* root samples collected in March 2022 (Table S6). The culture-dependent approach revealed notable differences in the microbial composition between *AP* and *GU*. In *AP*, we identified 16 bacterial species from 7 different orders and 7 fungal species from 4 orders. In contrast, *GU* exhibited relatively less diversity, with 11 bacterial species predominantly from the orders *Bacillales* and *Hyphomicrobiales*, and only 2 fungal species from 2 different orders. These findings highlight that distinct culturable microbial communities are associated with each plant. Specifically, *Pseudomonas extremorientalis* dominated the bacterial community in *AP*, comprising 16% of the relative abundance, whereas *Fusarium pseudoanthophilum* was the most prevalent fungal species, making up 30% of the fungal community. Conversely, in *GU*, *Bacillus cereus* represented 30.77% of the bacterial community, and *Paradictyoarthrinium aquatica*, belonging to the order *Pleosporales*, dominated the fungal community at 66.77%.

All 68 isolates were subjected to BLAST identification with culture-independent data. The reliability of the evaluation results was determined to be 97%. When BLAST analysis was performed with amplicon data, *Priestia megaterium*, *Pr. aryabhattai*, *B. cereus*, *B. paranthracis*, and *B. velezensis* showed over 97% match with bacteria belonging to the genus *Bacillus* (Table S7). When comparing our culture-independent results with our culture-dependent findings, we observed the presence of several bacterial and fungal species across both approaches. Specifically, among the bacterial species, we identified *Pseudomonas brassicacearum subsp. neoaurantiaca* AP-B26 (100% similarity), *Ps. frederiksbergensis* AP-B12 (99.735% similarity), *Ps. congelans* AP-B14, *Ps. caspiana* AP-B15 (99.471% similarity), and *Ps. extremorientalis* AP-B1, AP-B2, and AP-B18 (99.206% similarity). Among the fungi, *Paraphoma radicina* AP-F2 (99.6% similarity) and *Pa. radicina* AP-F5 (98.776% similarity) were detected. Moreover, unique microbial isolates were identified in *AP*. *Fusarium* and *Paraphoma* species were exclusively associated with *AP*, with B2_*Pseudomonas*, F786_*Fusarium*, F5_*Paraphoma*, and F28_*Paraphoma* showing differential abundance in culture-independent analyses. These findings further confirm the presence of these bacterial strains in both *AP* and *GU*, with certain strains, such as *B. cereus*, demonstrating a higher prevalence in *GU* than in *AP*.

Discussion

It is known that helpful and nonbeneficial bacterial and fungal endophytes are commonly found in plant roots. The elements that decide whether endophytes will be advantageous for the host plant, as well as the extrinsic cues involved and the dynamics of the plant-endophyte connection, are not fully elucidated. Herein, the results obtained during the examination of microbial community composition in *AP* and *GU* plants provide valuable novel insights into the complex connections between medicinal plants and microbes. Our findings reveal distinct microbial compositions and diversities within these two medicinal plants, emphasizing their unique microbial compositions, diversities, and intricate relationships among microbes. The dominance of specific bacterial genera, including *Bacillus*, *Pseudomonas*, and *Rhizobium*, along with the fungal communities predominantly comprising *Ascomycota* in *AP* and *Basidiomycota* in *GU*, highlights the selective nature of root microbiomes and their fundamental compositional differences in host plants (Chen et al., 2022).

The dominance of *Proteobacteria* in both *AP* and *GU*, although with different dominant orders (*Pseudomonadales* in *AP* and *Xanthomonadales* in *GU*), is consistent with the results of previous studies emphasizing the abundance of *Proteobacteria* in different plant-associated microbials. This prevalence can be attributed to the metabolic flexibility and adaptability of *Proteobacteria* (Compant et al., 2019; Franke-Whittle et al., 2015; Schlaeppi & Bulgarelli, 2015). The existence of distinct bacterial orders in both plant species, such as *Steroidobacterales* in *AP* and *Chlamydiales* in *GU*, indicates the presence of distinctive interactions between the host and microbes. The presence of these bacterial orders in *AP* and *GU* may impact the abundances and activities of *Steroidobacterales* and *Chlamydiales*, two groups of bacteria that play important roles in plant–microbe interactions. It has been reported that *Steroidobacterales*, a bacterial order present in *AP*, has the ability to produce antiproliferative and immunosuppressive compounds (Vurukonda et al., 2018). These interactions have the potential to affect

the physiological characteristics and stress responses of plants (Berendsen et al., 2012; Brencic & Winans, 2005; Etesami & Beattie, 2017). The results of our study emphasize the difference in composition, with *Ascomycota*, specifically *Pleosporales*, being the most abundant in *AP*, whereas *Basidiomycota*, particularly *Phallales*, being more prevalent in *GU*. Nevertheless, the notable occurrence of the order *Boletales* from the phylum *Basidiomycota* in both locations indicates an intricate interaction among these fungal communities. This distinct fungal composition has the potential to improve the ability of the host plant to withstand various challenges, potentially providing diverse benefits to the diversity observed in *AP* and *GU*, likely implying a unique preference for fungi that can affect the ability of the host plant to withstand infections and environmental stressors (Kutos et al., 2022; Vadakattu et al., 2017).

The notable differences in alpha diversity between the bacterial and fungal communities of *AP* and *GU* are of particular significance, particularly in light of the presence of *Bacillus* species within *GU*. The results of both culture-dependent and -independent analyses confirm the presence of *Bacillus* in *GU*, suggesting a potential key role for this genus in plant microbial. The bacterial community of *AP*, which exhibits greater alpha diversity than in *GU*, could enhance plant resilience and health by fostering a relatively more robust microbial community capable of combating diseases (Mendes et al., 2011), which is particularly relevant for *Bacillus cereus* G2, known to significantly improve the salt stress tolerance of licorice by enhancing its photosynthetic efficiency, carbohydrate metabolism, and the accumulation of medicinal compounds, such as glycyrrhizic acid and liquiritin (Zhang et al., 2022). The presence of *Bacillus* in *GU* may indicate a specialized adaptation, possibly contributing to the ability of the plant to thrive in specific environmental conditions. In contrast, the higher fungal alpha diversity in *GU* than in *AP* may suggest a varied fungal community that plays distinct ecological roles, potentially affecting nutrient cycling and soil health (Van Der Heijden et al., 2008). This diversity could reflect an intricate balance within the microbial, where bacteria like *Bacillus* work in tandem with fungi to support plant health. In our study, the proven presence of *Bacillus* in *GU*, particularly considering its crucial functions, raises possibilities regarding the interactions between bacterial and fungal communities and how these relationships could be leveraged to enhance plant resilience and productivity. This complex interplay between diverse microbial communities could be the key to understanding and optimizing plant–microbe interactions for improved agricultural outcomes.

An important discovery of our research is the identification of key microorganisms within the root microbiomes of *AP* and *GU*. The core ASVs, which are consistently present in different samples, have crucial functions in the operation of the community and emphasize the stable elements of the microbiome associated with plants. In our study, the specific members of *Proteobacteria* and *Actinobacteria*, such as B70_*Cutibacterium*, B5_f_*Comamonadaceae*, and B2_f_*Pseudomonas*, have been identified as the core ASVs of *AP* and *GU*. Studies have demonstrated that the microorganisms present in medicinal plants, such as *Comamonadaceae* and *Pseudomonas*, have a substantial impact on the production of bioactive substances, such as glycyrrhizin, which, in turn, enhances the therapeutic benefits of these plants (Abd Aziz et al., 2021). A key characteristic of *Comamonadaceae* is their adaptability to different environmental conditions. They have been isolated from both polluted and

pristine environments, showcasing their ability to thrive in a variety of habitats. Furthermore, they have been found to interact symbiotically with plants, promoting growth and providing protection against pathogens (Sah et al., 2021). The widespread occurrence of *Comamonadaceae* can be attributed to their physiological and genetic diversity, which enables them to colonize and adapt to diverse ecological niches. They have been observed to form vibrant assemblages with other beneficial microbes, such as *Pseudomonas* spp., in the rhizosphere, creating a mutually beneficial relationship with the host plant (Sah et al., 2021). Exploring the potential overlap between the niches occupied by the *Comamonadaceae* species and the production of primary plant nutrients, such as carbohydrates, may provide valuable insights into the intricate interactions between these plants and their associated microbiomes (Andreote et al., 2014). Additionally, *Actinobacteria* has been found in enriched amounts in the rhizosphere, soil, and root of *GU* (Chen et al., 2022). Further research into specific microbial species within the core ASVs and their metabolic activities is suggested to harness these beneficial plant–microbe interactions (Chen et al., 2022; Qiao et al., 2018). These findings can facilitate the development of bioengineering techniques to improve the therapeutic characteristics of plants through favorable interactions with microbial communities (Andreote et al., 2014; Lareen et al., 2016; Niu et al., 2017; Trivedi et al., 2020).

The results of the network analysis provide valuable insights into the intricate relationships within the endophytic microbial communities of *AP* and *GU*. Hubs that are highly connected and effective play a crucial role in shaping microbial assembly and enhancing biodiversity. The presence of these hub taxa is also impacted by the physicochemical parameters of the rhizospheric soil (Mora-Ruiz et al., 2016). In case of halophytes, such as *Salicornia europaea*, the endophytic bacterial and fungal communities are determined by the origin of salinity at the sites, with the bacterial community impacting the fungal community (Furtado et al., 2019). The finding of hub nodes in both plants highlights the central key within these microbial networks that can have a substantial impact on plant growth and health. In our study, B152_o_*Burkholderiales*, F14_*Exophiala*, and F33_*Fusarium* were identified as key hub nodes in *AP*, whereas B36_*Paenibacillus* emerged as an important key hub node in *GU*. Although there is limited specific research on these taxa in the context of *AP* and *GU*, studies in other plants suggest that *Burkholderiales* species are often involved in promoting plant growth and resistance against pathogens (Kang et al., 2012). Similarly, *Exophiala* spp. have been shown to be associated with endophytic traits that may enhance plant stress tolerance (Khan et al., 2011), and *Fusarium* is known for its dual role as a pathogen and a potential plant growth-promoting microorganism (Patel et al., 2022) under certain conditions. These findings support the hypothesis that the identified hub ASVs may also play similar roles in *AP* and *GU* and potentially contribute to plant health and resilience. Moreover, these findings identify important points in the microbial control of plants, offering a comprehensive view of the potential effects of these microbial networks. Gaining knowledge regarding these interactions can be a foundation for altering microbial communities to enhance plant resistance and productivity (Agler et al., 2016; Sturz & Nowak, 2000; Tao et al., 2018).

The observation that *AP* and *GU* plants host distinct microbial communities within their root microbials is corroborated by both culture-dependent and -independent analyses. Notably, in *AP*, microorganisms, such as *Ps. extremorientalis* (16%) and *Fu. pseudoanthophilum* (30%) were found to be abundant when

assessed using culture-dependent methods, suggesting that *AP* may have a relatively more diverse microbial community. Furthermore, culture-independent approaches revealed that *Fusarium* and *Paraphoma* spp. were specific to *AP*, suggesting that these microorganisms are relatively more prevalent in this plant and may form symbiotic relationships that enhance plant health. This unique microbial association could potentially confer improved resistance to environmental stresses or pathogenic attacks for *AP*. In contrast, the predominance of *B. cereus* and *Par. aquatica* in the *GU* microbial indicates a narrower microbial diversity, with a symbiotic community largely based on *Bacillus* spp. Antibiotics and enzymes produced by *Bacillus*, can promote improved growth by suppressing plant pathogens, thereby increasing the yield of bioactive compounds, such as polysaccharides and saponins (Lin et al., 2022; Sun et al., 2017). The microbial communities associated with *AP* and *GU* may play a significant role in shaping their phytochemical profiles. For instance, glycyrrhizin and astragalosides, key metabolites in *GU* and *AP*, could be impacted by the metabolic activities of associated microorganisms (Abd Aziz et al., 2021; Li, Liu, et al., 2021). Microbes, such as *Pseudomonas* and *Cladosporium*, identified in this study, are known producers of bioactive compounds that could impact plant metabolic pathways (Chandra et al., 2024). *Pseudomonas* spp. may be capable of producing phenazines and siderophores, which may enhance nutrient uptake or signaling processes in plants (Biessy & Filion, 2018). Similarly, *Cladosporium* spp. may be associated with the production of antioxidant phenolic compounds (Chandra et al., 2024). These findings suggest that both *AP* and *GU* selectively favor distinct microbial communities, each with a unique composition, which may have significant implications for their health and growth.

Our research adds to the expanding knowledge base on plant-associated microbiomes, providing novel perspectives on the microbial communities and their organization in *AP* and *GU* medicinal plants. The unique microbial profiles discovered in these plants highlight the significance of specialized host–microbe interactions in impacting plant health, growth, and therapeutic properties. Future studies must focus on elucidating the practical consequences of these microbial relationships, which will help in devising strategies for effectively managing microorganisms in the cultivation and breeding of these medicinal plants.

Abbreviations

AP: *Astragalus propinquus*

GU: *Glycyrrhiza uralensis*

PBS: phosphate-buffered saline

ISP5: ISP Medium No. 5 (glycerol–asparagine agar base)

ISP2: ISP Agar 2 (yeast extract–malt extract agar)

EYA: egg yolk agar

LB: Luria–Bertani agar

TSA: trypticase soy agar

R2A: Reasoner’s 2A agar

YPDA: yeast peptone dextrose adenine

MPDA: MEDION potato dextrose agar

PDA: potato dextrose agar

RBA: rose bengal agar

SDA: Sabouraud dextrose agar

CFU: colony-forming unit

PCR: polymerase chain reaction

DNA: deoxyribose nucleic acid

NCBI: National Center for Biotechnology Information

Declarations

Additional Information

Publisher’s Note

Springer Nature remains neutral with regard to jurisdictional claims in published maps and institutional affiliations.

Supplementary Files

Supplementary file 1

Supplementary Table 1

Supplementary Table 2

Supplementary Table 3

Supplementary Table 4

Supplementary Table 5

Supplementary Table 6

Supplementary Table 7

Ethics approval and consent to participate

Not applicable.

Consent for publication

Not applicable.

Availability of data and materials

All raw sequences derived from this experiment were submitted to the Sequence Read Archive of NCBI and can be found under the Bio Project accession numbers PRJNA1093218 (*AP*) and PRJNA1093232 (*GU*). Analysis codes are available from (https://github.com/papican).

Competing interests

The authors declare no conflict of interest.

Funding

This work was supported by the National Research Foundation of Korea grants funded by the Korean Government (MSIT) (2018R1A5A1023599, 2021M3H9A1096935, and RS-2023-00275965 to Y.-H.L. and 2022R1C1C2002739 to H.K.).

Author contributions

ZKK and Y-HL conceived and planned the experiment. ZKK performed public data analyses and wrote the original draft. YSP and T-JY collected plant samples. ZKK, and HK contributed to the preparation of the manuscript. ZKK, HK, and Y-HL contributed to manuscript editing and finalization. All authors contributed to the article and approved the submitted version.

Acknowledgements

Not applicable.

References

1. Abd Aziz NA, Hasham R, Sarmidi MR, Suhaimi SH, Idris MKH (2021) A review on extraction techniques and therapeutic value of polar bioactives from Asian medicinal herbs: Case study on *Orthosiphon aristatus*, *Eurycoma longifolia* and *Andrographis paniculata*. Saudi Pharm J 29(2):143-65. https://doi.org/10.1016/j.jsps.2020.12.016

2. Agler MT, Ruhe J, Kroll S, Morhenn C, Kim S-T, Weigel D et al. (2016) Microbial hub taxa link host and abiotic factors to plant microbiome variation. PLoS Biol 14(1):e1002352. https://doi.org/10.1371/journal.pbio.1002352
3. Andreote FD, Gumiere T, Durrer A (2014) Exploring interactions of plant microbiomes. Sci Agric 71:528-39. https://doi.org/10.1590/0103-9016-2014-0195
4. Asl MN, Hosseinzadeh H (2008) Review of pharmacological effects of *Glycyrrhiza* sp. and its bioactive compounds. Phytother Res 22(6):709-24. https://doi.org/10.1002/ptr.2362
5. Bakker PA, Berendsen RL, Doornbos RF, Wintermans PC, Pieterse CM (2013) The rhizosphere revisited: root microbiomics. Front Plant Sci 2013;4:165. https://doi.org/10.3389/fpls.2013.00165
6. Bastian M, Heymann S, Jacomy M (2009) Gephi: An open source software for exploring and manipulating networks. ICWSM 3(1):361-2. https://doi.org/10.1609/icwsm.v3i1.13937
7. Berendsen RL, Pieterse CM, Bakker PA (2012) The rhizosphere microbiome and plant health. Trends Plant Sci 17(8):478-86. https://doi.org/10.1016/j.tplants.2012.04.001
8. Biessy A, Filion M (2018). Phenazines in plant-beneficial *Pseudomonas* spp.: biosynthesis, regulation, function and genomics. Environ Microbiol, 20(11), 3905-3917. https://doi.org/10.3389/fmicb.2021.642730
9. Bokulich NA, Kaehler BD, Rideout JR, Dillon M, Bolyen E, Knight R, et al. (2018) Optimizing taxonomic classification of marker-gene amplicon sequences with QIIME 2's q2-feature-classifier plugin. Microbiome 6(1):1-17. https://doi.org/10.1186/s40168-018-0470-z
10. Bolyen E, Rideout JR, Dillon MR, Bokulich NA, Abnet CC, Al-Ghalith GA et al. (2019) Reproducible, interactive, scalable and extensible microbiome data science using QIIME 2. Nat Biotechnol 37(8):852-7. https://doi.org/10.1038/s41587-019-0209-9
11. Brader G, Compant S, Mitter B, Trognitz F, Sessitsch A (2014) Metabolic potential of endophytic bacteria. Curr Opin Biotechnol 27:30-7. https://doi.org/10.1016/j.copbio.2013.09.012
12. Bratkov VM, Shkondrov AM, Zdraveva PK, Krasteva IN (2016) Flavonoids from the genus *Astragalus*: phytochemistry and biological activity. Pharmacogn Rev 10(19):11. https://doi.org/10.4103/0973-7847.176550
13. Brencic A, Winans SC (2005) Detection of and response to signals involved in host-microbe interactions by plant-associated bacteria. Microbiol Mol Biol Rev 69(1):155-94. https://doi.org/10.1128/MMBR.69.1.155-194.2005
14. Bulgarelli D, Rott M, Schlaeppi K, Ver Loren van Themaat E, Ahmadinejad N, Assenza F et al. (2012) Revealing structure and assembly cues for *Arabidopsis* root-inhabiting bacterial microbiota. Nature 488(7409):91-5. https://doi.org/10.1038/nature11336
15. Callahan BJ, McMurdie PJ, Rosen MJ, Han AW, Johnson AJA, Holmes SP (2016) DADA2: High-resolution sample inference from Illumina amplicon data. Nat Methods 13(7):581-3. https://doi.org/10.1038/nmeth.3869
16. Chandra H, Yadav A, Prasad R, Kalra SJS, Singh A, Bhardwaj N, et al. (2024) Fungal endophytes from medicinal plants acting as natural therapeutic reservoir. The Microbe 2024:100073.

https://doi.org/10.1016/j.microb.2024.100073

17. Chaparro JM, Badri DV, Vivanco JM (2014) Rhizosphere microbiome assemblage is affected by plant development. ISME J 8(4):790-803. https://doi.org/10.1038/ismej.2013.196
18. Chaparro JM, Sheflin AM, Manter DK, Vivanco JM (2012) Manipulating the soil microbiome to increase soil health and plant fertility. Biol Fertil Soils 48:489-99. https://doi.org/10.1007/s00374-012-0691-4
19. Chen C, Zhong C, Gao X, Tan C, Bai H, Ning K (2022) *Glycyrrhiza uralensis* Fisch. Root-associated microbiota: the multifaceted hubs associated with environmental factors, growth status and accumulation of secondary metabolites. Environ Microbiome 17(1):23. https://doi.org/10.1186/s40793-022-00418-0
20. Chung WT, Lee SH, Kim JD, Sung NS, Hwang B, Lee SY, et al. (2001) Effect of the extracts from *Glycyrrhiza uralensis* Fisch on the growth characteristics of human cell lines: Anti-tumor and immune activation activities. Cytotechnology 37:55-64. https://doi.org/10.1023/A:1016111713056
21. Compant S, Samad A, Faist H, Sessitsch A (2019) A review on the plant microbiome: ecology, functions, and emerging trends in microbial application. J Adv Res 19:29-37. https://doi.org/10.1016/j.jare.2019.03.004
22. del Carmen Orozco-Mosqueda M, del Carmen Rocha-Granados M, Glick BR, Santoyo G (2018) Microbiome engineering to improve biocontrol and plant growth-promoting mechanisms. Microbiol Res 208:25-31. https://doi.org/10.1016/j.micres.2018.01.005
23. Deng Z, Cao L (2017) Fungal endophytes and their interactions with plants in phytoremediation: a review. Chemosphere 168:1100-6. https://doi.org/10.1016/j.chemosphere.2016.10.097
24. Etesami H, Beattie GA (2017) Plant-microbe interactions in adaptation of agricultural crops to abiotic stress conditions. In: Kumar, V., Kumar, M., Sharma, S., Prasad, R. (eds) Probiotics and Plant Health. Springer, Singapore. https://doi.org/10.1007/978-981-10-3473-2_7
25. Feng K, Peng X, Zhang Z, Gu S, He Q, Shen W et al. (2022) iNAP: An integrated network analysis pipeline for microbiome studies. iMeta 1(2):e13. https://doi.org/10.1002/imt2.13
26. Franke-Whittle IH, Manici LM, Insam H, Stres B (2015) Rhizosphere bacteria and fungi associated with plant growth in soils of three replanted apple orchards. Plant Soil 395:317-33. https://doi.org/10.1007/s11104-015-2562-x
27. Friedman J, Alm EJ (2012) Inferring correlation networks from genomic survey data. PLoS Comput Biol 8(9): e1002687. https://doi.org/10.1371/journal.pcbi.1002687
28. Furtado BU, Gołębiewski M, Skorupa M, Hulisz P, Hrynkiewicz K (2019) Bacterial and fungal endophytic microbiomes of *Salicornia europaea*. Appl Environ Microbiol 85(13):e00305-19. https://doi.org/10.1128/AEM.00305-19
29. Hassani MA, Durán P, Hacquard S (2018) Microbial interactions within the plant holobiont. Microbiome 6:1-17. https://doi.org/10.1186/s40168-018-0445-0
30. Huang W, Long C, Lam E (2018) Roles of plant-associated microbiota in traditional herbal medicine. Trends Plant Sci 23(7):559-62. https://doi.org/10.1016/j.tplants.2018.05.003

31. Ji S Li, Z Song W, Wang Y, Liang W, Li K, Tang S et al. (2016). Bioactive constituents of *Glycyrrhiza uralensis* (licorice): discovery of the effective components of a traditional herbal medicine. J Nat Prod, 79(2), 281-292. https://doi.org/10.1021/acs.jnatprod.5b00877
32. Kang SM, Khan AL, Hussain J, Ali L, Kamran M, Waqas et al. (2012) Rhizonin A from *Burkholderia* sp. KCTC11096 and its growth promoting role in lettuce seed germination. Molecules 17(7), 7980-7988. https://doi.org/10.3390/molecules17077980
33. Khan AL, Hamayun M, Ahmad N, Waqas M, Kang SM, Kim YH et al. (2011) *Exophiala* sp. LHL08 reprograms *Cucumis sativus* to higher growth under abiotic stresses. Physiol Plant 143(4), 329-343. https://doi.org/10.1111/j.1399-3054.2011.01508.x
34. Kudjordjie EN, Sapkota R, Steffensen SK, Fomsgaard IS, Nicolaisen M (2019) Maize synthesized benzoxazinoids affect the host associated microbiome. Microbiome 7(1):1-17. https://doi.org/10.1186/s40168-019-0677-7
35. Kurtz ZD, Müller CL, Miraldi ER, Littman DR, Blaser MJ, Bonneau RA (2015) Sparse and compositionally robust inference of microbial ecological networks. PLoS Comput Biol 11(5):e1004226. https://doi.org/10.1371/journal.pcbi.1004226
36. Kutos S, Barnes EM, Bhutada A, Lewis J (2022) Preferential associations of soil fungal taxa under mixed compositions of eastern American tree species. FEMS Microbiol Ecol 98(6):fiac056. https://doi.org/10.1093/femsec/fiac056
37. Lane D (1991) 16S/23S rRNA Sequencing. In: Stackebrandt, E Goodfellow, M (ed), Nucleic acid techniques in bacterial systematic, John Wiley and Sons, Chichester, UK.
38. Lareen A, Burton F, Schäfer P (2016) Plant root-microbe communication in shaping root microbiomes. Plant Mol Biol. 90:575-87. https://doi.org/10.1007/s11103-015-0417-8
39. Lebeis SL (2014) The potential for give and take in plant–microbiome relationships. Front Plant Sci 5:287. https://doi.org/10.3389/fpls.2014.00287
40. Lee S, Malone C, Kemp PF (1993) Use of multiple 16S rRNA-targeted fluorescent probes to increase signal strength and measure cellular RNA from natural planktonic bacteria. Mar Ecol Prog Ser 193-201. https://doi.org/10.3354/meps101193
41. Li Y, Liu Y, Zhang H, Yang Y, Wei G, Li Z (2021). The composition of root-associated bacteria and fungi of *Astragalus mongholicus* and their relationship with the bioactive ingredients. Front Microbiol 12, 642730. https://doi.org/10.3389/fmicb.2021.642730
42. Li Y, Yang Y, Zhang H, Wei G, Li Z (2021) Rhizosphere bacterial and fungal spatial distribution and network pattern of *Astragalus mongholicus* in representative planting sites differ the bulk soil. Appl Soil Ecol 168:104114. https://doi.org/10.1016/j.apsoil.2021.104114
43. Liaw A, Wiener M (2002) Classification and regression by randomForest. R news. 2(3):18-22. Vol. 2/3, December 2002
44. Liu Y-t, Lv W-l (2020) Research progress in *Astragalus membranaceus* and its active components on immune responses in liver fibrosis. Chin J Integr Med 26(10):794-800. https://doi.org/10.1007/s11655-019-3039-1

45. Liu Z, Ma Y, Lv X, Li N, Li X, Xing J et al. (2023) Abiotic factors and endophytes co-regulate flavone and terpenoid glycoside metabolism in *Glycyrrhiza uralensis*. Appl Microbiol Biotechnol 107(7):2671-88. https://doi.org/10.1007/s00253-023-12441-3
46. Ludwig-Müller J (2015) Plants and endophytes: equal partners in secondary metabolite production? Biotechnol Lett 37:1325-34. https://doi.org/10.1007/s10529-015-1814-4
47. Marasco R, Rolli E, Ettoumi B, Vigani G, Mapelli F, Borin S et al. (2012) A drought resistance-promoting microbiome is selected by root system under desert farming. PLoS ONE 7(10):e48479. https://doi.org/10.1371/journal.pone.0048479
48. Masand M, Jose PA, Menghani E, Jebakumar SRD (2015) Continuing hunt for endophytic actinomycetes as a source of novel biologically active metabolites. World J Microbiol Biotechnol 31:1863-75. https://doi.org/10.1007/s11274-015-1950-y
49. McMurdie PJ, Holmes S (2013) phyloseq: an R package for reproducible interactive analysis and graphics of microbiome census data. PLoS ONE 8(4):e61217. https://doi.org/10.1371/journal.pone.0061217
50. Mendes R, Kruijt M, De Bruijn I, Dekkers E, Van Der Voort M, Schneider JH et al. (2011) Deciphering the rhizosphere microbiome for disease-suppressive bacteria. Science 332(6033):1097-100. https://doi.org/10.1126/science.1203980
51. Mora-Ruiz MdR, Font-Verdera F, Orfila A, Rita J, Rosselló-Móra R (2016) Endophytic microbial diversity of the halophyte *Arthrocnemum macrostachyum* across plant compartments. FEMS Microbiol Ecol 92(9):fiw145. https://doi.org/10.1093/femsec/fiw145
52. Müller DB, Vogel C, Bai Y, Vorholt JA (2016) The plant microbiota: systems-level insights and perspectives. Annu Rev Genet 50:211-34. https://doi.org/10.1146/annurev-genet-120215-034952
53. Nilsson RH, Larsson K-H, Taylor AFS, Bengtsson-Palme J, Jeppesen TS, Schigel D et al. (2019) The UNITE database for molecular identification of fungi: handling dark taxa and parallel taxonomic classifications. Nucleic Acids Res 47(D1):D259-D64. https://doi.org/10.1093/nar/gky1022
54. Niu B, Paulson JN, Zheng X, Kolter R (2017) Simplified and representative bacterial community of maize roots. Proc Natl Acad Sci U S A 114(12):E2450-E9. https://doi.org/10.1073/pnas.1616148114
55. Oksanen J, Blanchet FG, Kindt R, Legendre P, Minchin PR, O'Hara, et al. (2014) Vegan: Community Ecology Package. R Package Version 2.2-0. https://cran.r-project.org/web/packages/vegan/index.html.
56. Oono R, Lefèvre E, Simha A, Lutzoni F (2015) A comparison of the community diversity of foliar fungal endophytes between seedling and adult loblolly pines (*Pinus taeda*). Fungal Biol 119(10):917-28. https://doi.org/10.1016/j.funbio.2015.07.003
57. Op De Beeck M, Lievens B, Busschaert P, Declerck S, Vangronsveld J, Colpaert JV (2014) Comparison and validation of some ITS primer pairs useful for fungal metabarcoding studies. PLoS ONE 9(6):e97629. https://doi.org/10.1371/journal.pone.0097629
58. Patel R, Mehta K, Prajapati J, Shukla A, Parmar P, Goswami D et al. (2022). An anecdote of mechanics for Fusarium biocontrol by plant growth promoting microbes. BioControl 174, 105012.

https://doi.org/10.1016/j.biocontrol.2022.105012

59. Paulson JN, Stine OC, Bravo HC, Pop M (2013) Differential abundance analysis for microbial marker-gene surveys. Nat Methods 10(12):1200-2. https://doi.org/10.1038/nmeth.2658
60. Qiao H, Zhang L, Shi H, Song Y, Bian C (2018) Astragalus affects fecal microbial composition of young hens as determined by 16S rRNA sequencing. AMB Express 8:1-10. https://doi.org/10.1186/s13568-018-0600-9
61. Quast C, Pruesse E, Yilmaz P, Gerken J, Schweer T, Yarza P et al. (2012) The SILVA ribosomal RNA gene database project: improved data processing and web-based tools. Nucleic Acids Res 41(D1):D590-D6. https://doi.org/10.1093/nar/gks1219
62. Ritchie ME, Phipson B, Wu D, Hu Y, Law CW, Shi W et al. (2015) limma powers differential expression analyses for RNA-sequencing and microarray studies. Nucleic Acids Res 43(7):e47-e. https://doi.org/10.1093/nar/gkv007
63. Sah S, Krishnani S, Singh R (2021). *Pseudomonas* mediated nutritional and growth promotional activities for sustainable food security. Curr Res Microb Sci 2,100084. https://doi.org/10.1016/j.crmicr.2021.100084
64. Schlaeppi K, Bulgarelli D (2015) The plant microbiome at work. Mol Plant Microbe Interact 28(3):212-7. https://doi.org/10.1094/MPMI-10-14-0334-FI
65. Stickel F, Schuppan D (2007) Herbal medicine in the treatment of liver diseases. Dig Liver Dis 39(4):293-304. https://doi.org/10.1016/j.dld.2006.11.004
66. Sturz A, Nowak J (2000) Endophytic communities of rhizobacteria and the strategies required to create yield enhancing associations with crops. Appl Soil Ecol 15(2):183-90. https://doi.org/10.1016/S0929-1393(00)00094-9
67. Sun H, Kang B, Chai Z, Sun H, Du H, Gao J et al. (2017) Characterization of root-associated microbiota in medicinal plants *Astragalus membranaceus* and *Astragalus mongholicus*. Ann Microbiol 67, 587-599. https://doi.org/10.1007/s13213-017-1285-z
68. Sun Y-g, Li J, Zhang Q-H, Guo X-R, Zhang B-l, Jin H (2012) The experimental study of *Astragalus membranaceus* on meridian tropsim: the distribution study of astragaloside IV in rat tissues. J Chromatogr B Analyt Technol Biomed Life Sci 911:71-5. https://doi.org/10.1016/j.jchromb.2012.10.024
69. Tao J, Meng D, Qin C, Liu X, Liang Y, Xiao Y et al. (2018) Integrated network analysis reveals the importance of microbial interactions for maize growth. Appl Microbiol Biotechnol 102:3805-18. https://doi.org/10.1007/s00253-018-8837-4
70. Trivedi P, Leach JE, Tringe SG, Sa T, Singh BK (2020) Plant–microbiome interactions: from community assembly to plant health. Nat Rev Microbiol 18(11):607-21. https://doi.org/10.1038/s41579-020-0412-1
71. Turner TR, James EK, Poole PS (2013) The plant microbiome. Genome Biol 14(6):1-10. https://doi.org/10.1186/gb-2013-14-6-209

72. Uroz S, Courty PE, Oger P (2019) Plant symbionts are engineers of the plant-associated microbiome. Trends Plant Sci 24(10):905-16. https://doi.org/10.1016/j.tplants.2019.06.008
73. Vadakattu G, Smith L, Scheikowski L, Hunter G, Greenfield P (2017) Region-based differences in the diversity and abundance of fungal community in cotton soils. In: Cotton Research Conference, Canberra, 5-7 September 2017.
74. Van Der Heijden MG, Bardgett RD, Van Straalen NM (2008) The unseen majority: soil microbes as drivers of plant diversity and productivity in terrestrial ecosystems. Ecol Lett 11(3):296-310. https://doi.org/10.1111/j.1461-0248.2007.01139.x
75. Vurukonda SSKP, Giovanardi D, Stefani E (2018) Plant growth promoting and biocontrol activity of *Streptomyces* spp. as endophytes. Int J Mol Sci 19(4):952. https://doi.org/10.3390/ijms19040952
76. White TJ, Bruns T, Lee SH, Taylor JW (1990) Amplification and direct sequencing of fungal ribosomal RNA genes for phylogenetics. In: Innis MA, Gelfand DH, Sninsky JJ, White TJ. (eds) In: PCR protocols. London: Academic Press. p. 315-322. https://doi.org/10.1016/B978-0-12-372180-8.50042-1
77. Wickham H (2009) Elegant graphics for data analysis (ggplot2). New York: Springer-Verlag.
78. Xu F, Zhang Y, Xiao S, Lu X, Yang D, Yang X et al. (2006) Absorption and metabolism of *Astragali radix* decoction: in silico, in vitro, and a case study in vivo. Drug Metab Dispos 34(6):913-24. https://doi.org/10.1124/dmd.105.008300
79. Yoon S-H, Ha S-M, Kwon S, Lim J, Kim Y, Seo H et al. (2017) Introducing EzBioCloud: a taxonomically united database of 16S rRNA gene sequences and whole-genome assemblies. Int J Syst Evol Microbiol 67(5):1613-7. https://doi.org/10.1099/ijsem.0.001755
80. Zhang Y, Lang D, Zhang W, Zhang X (2022) *Bacillus cereus* enhanced medicinal ingredient biosynthesis in *Glycyrrhiza uralensis* Fisch. under different conditions based on the transcriptome and polymerase chain reaction analysis. Front Plant Sci 13:858000. https://doi.org/10.3389/fpls.2022.858000
81. Zhang Y, Zheng L, Zheng Y, Xue S, Zhang J, Huang P et al. (2020) Insight into the assembly of root-associated microbiome in the medicinal plant *Polygonum cuspidatum*. Ind Crops Prod 145:112163. https://doi.org/10.1016/j.indcrop.2020.112163
82. Zhu D, Wang J, Zeng Q, Zhang Z, Yan R (2010) A novel endophytic Huperzine A–producing fungus, *Shiraia* sp. Slf14, isolated from *Huperzia serrata*. J Appl Microbiol 109(4):1469-78. https://doi.org/10.1111/j.1365-2672.2010.04777.x

Figures

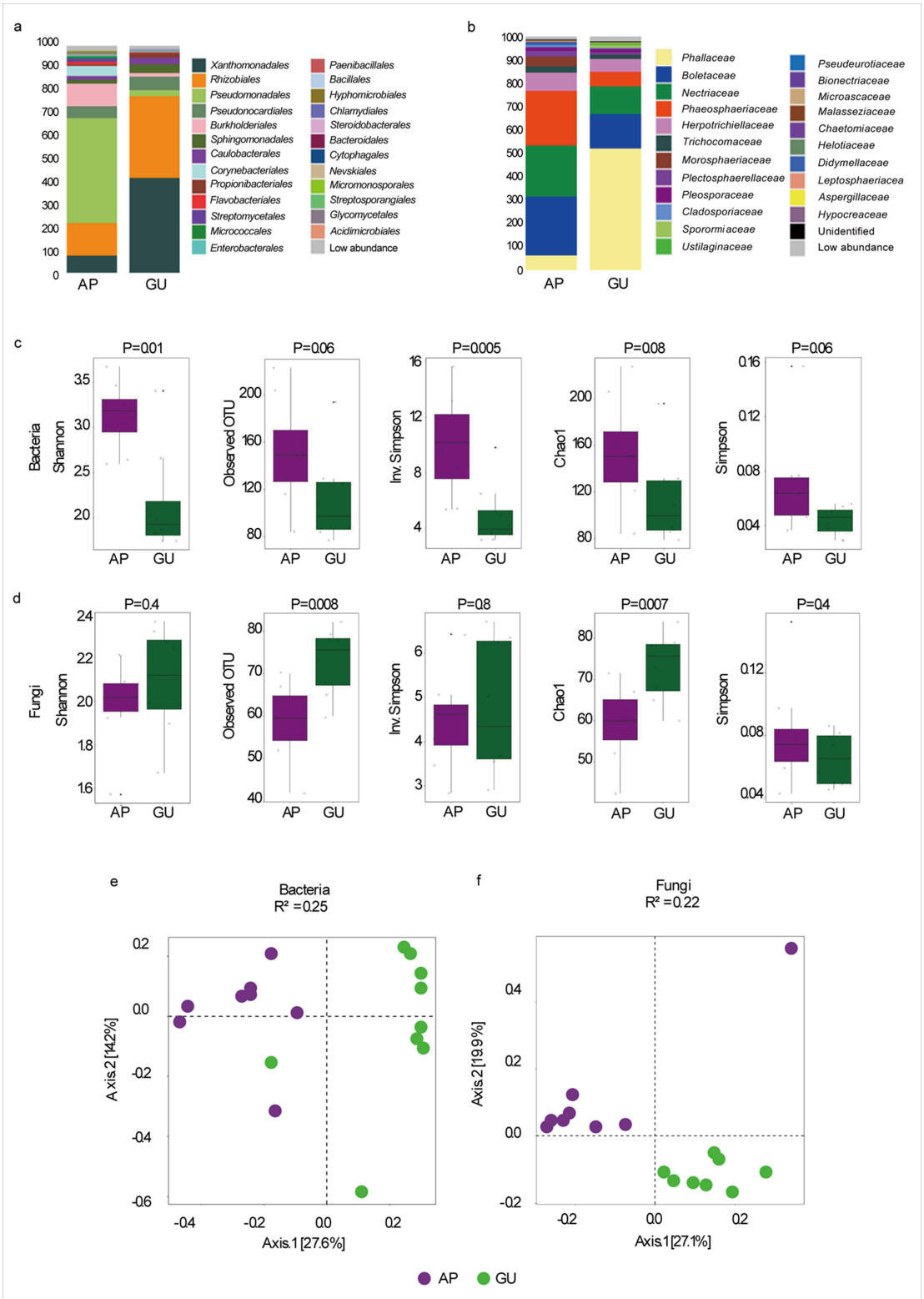


Figure 1

Relative abundance in the (a) bacterial and (b) fungal order, in the *Astragalus propinquus* (*AP*), and *Glycyrrhiza uralensis* (*GU*). Low abundance taxonomic groups with less than 5‰ (permille) of each sample are represented in gray. Unidentified taxonomic groups are indicated in black. The *p*-values for alpha diversity were calculated using the Wilcoxon rank-sum test (c, d). Cumulative sum scaling/log

transformed reads were used to calculate Bray–Curtis distances. Each point represents each sample replicate and was colored by plant species (purple for *AP*; green for *GU*) (e, f).

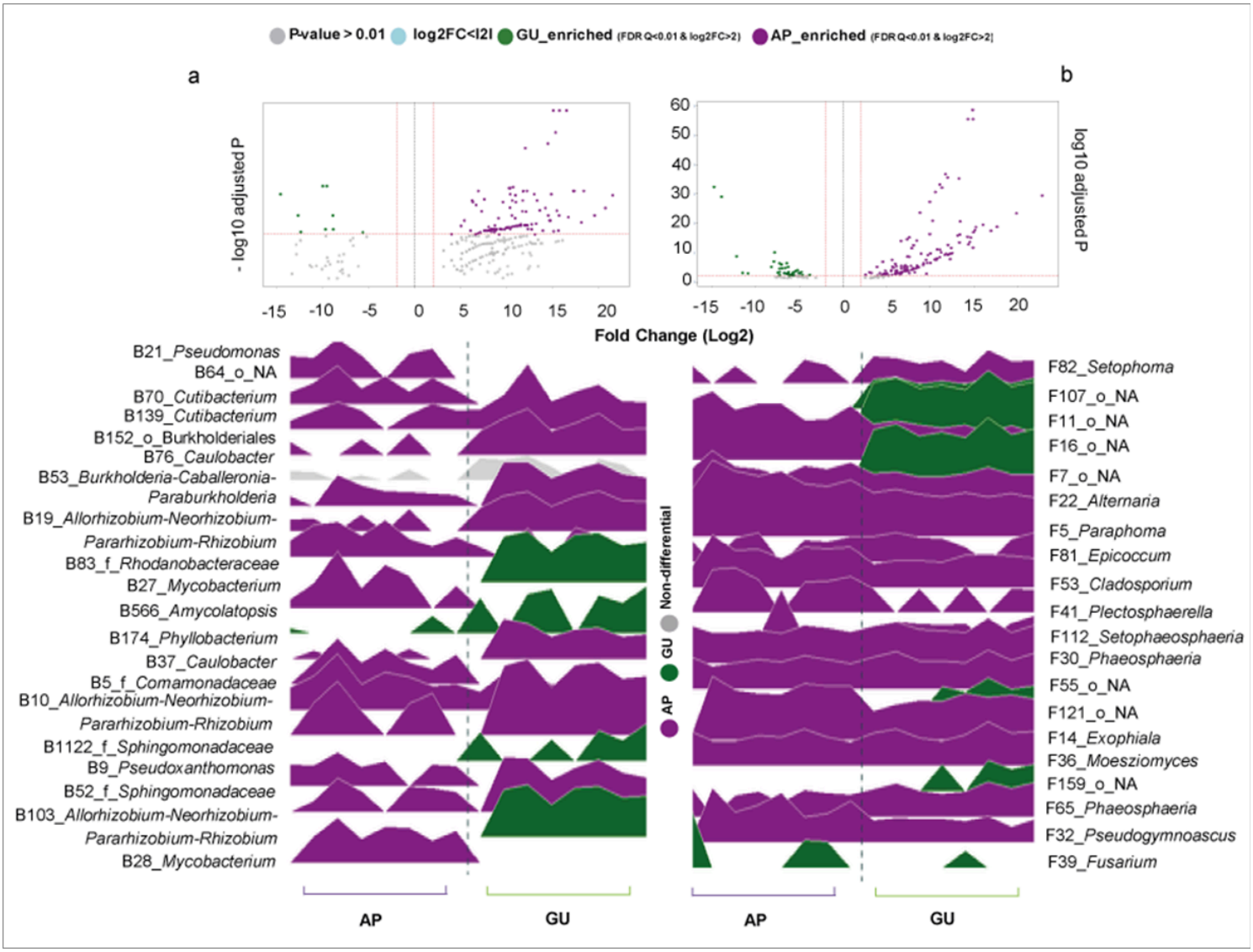


Figure 2

Differential abundance test and random forest classification to identify the amplicon sequence variants (ASVs) responsible for differences between the microbial of *Astragalus propinquus* (*AP*) and *Glycyrrhiza uralensis* (*GU*). Volcano plots were created to visualize the differentially abundant bacterial and fungal ASVs. To compare the microbial communities of the two plant species, we utilized a zero-inflated Gaussian distribution mixture model on ASV abundance tables normalized using cumulative sum scaling. The analysis included data from all eight replicates of each plant. The top 20 bacterial and fungal ASVs that most optimally discriminated between *AP* and *GU* were determined using a random forest classifier. The importance of each ASV in contributing to the accuracy of *AP* and *GU* prediction in the random forest model was ranked by calculating the mean decrease in the Gini impurity coefficient.

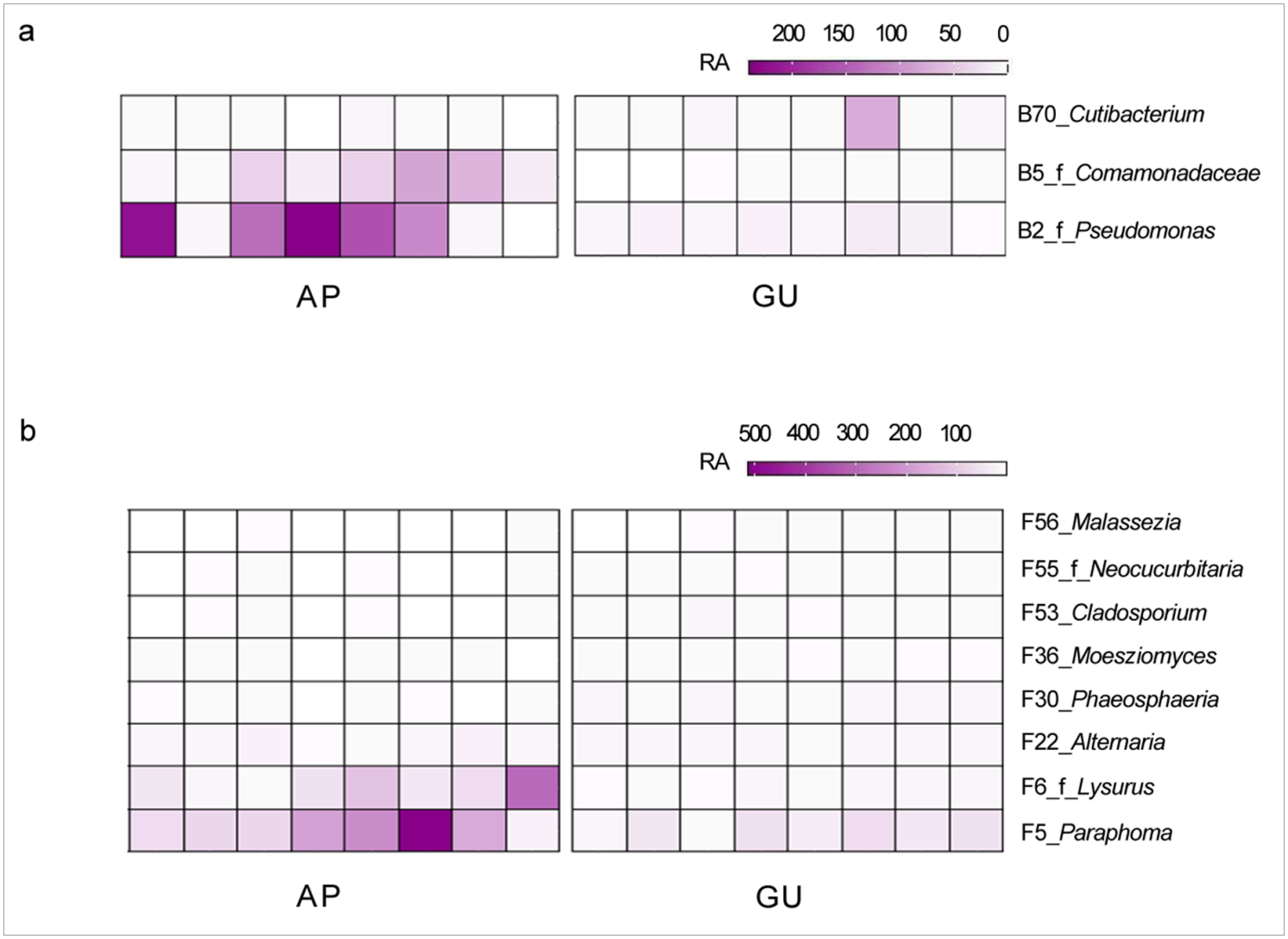


Figure 3

Heatmap representation of *Astragalus propinquus* (*AP*) and *Glycyrrhiza uralensis* (*GU*) core amplicon sequence variants (ASVs) showing the frequency of each ASV. The prevalence threshold for core ASV was 90% (bacteria) and 95% (fungi). RA, relative abundance.

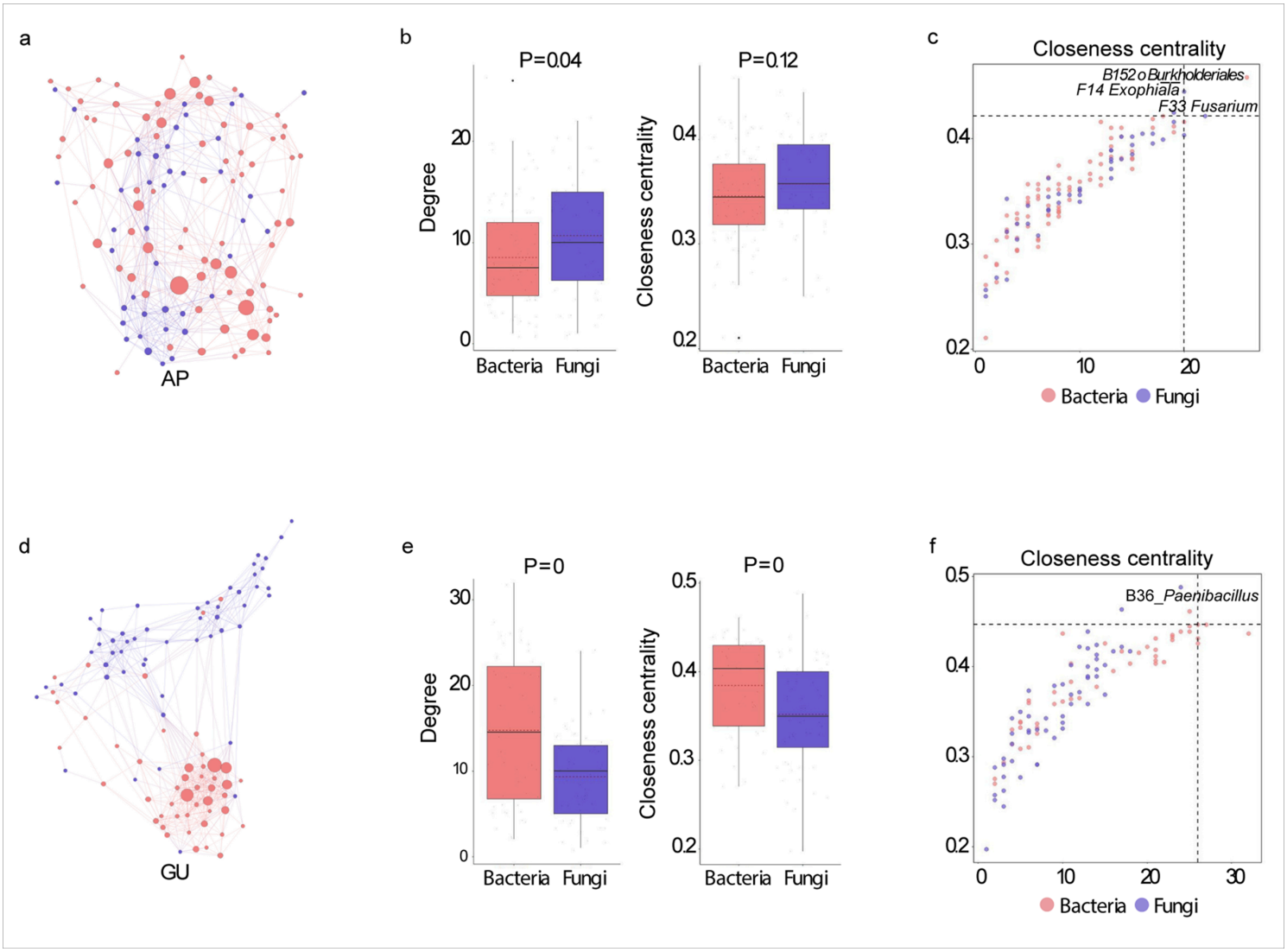


Figure 4

Co-occurrence-based network of *Astragalus propinquus* (*AP*) and *Glycyrrhiza uralensis* (*GU*) microbial amplicon sequence variants (ASVs) is detected. Each node corresponds to an ASV, and edges between nodes correspond to positive or negative correlations inferred from ASV abundance profiles using the SparCC method. ASVs belonging to bacteria are shown in light pink, fungi are shown in purple, and node size reflects their eigenvector centrality in *AP* and *GU*.

Supplementary Files

This is a list of supplementary files associated with this preprint. Click to download.

- Supplementaryfile1.docx
- SupplementaryfileS1.tif
- SupplementaryfileS2.tif
- SupplementaryfileTableS1.xlsx

- SupplementaryfileTableS2.xlsx
- SupplementaryfileTableS3.xlsx
- SupplementaryfileTableS4.xlsx
- SupplementaryfileTableS5.xlsx
- SupplementaryfileTableS6.xlsx
- SupplementaryfileTableS7.xlsx